

Improving Fuel Usage in Microchannel Based Fuel Cells

Petru S. Fodor and Joseph D'Alessandro
Physics Department, Cleveland State University
*Corresponding author: Petru S. Fodor, Physics Department, Cleveland State University, 2121 Euclid Avenue, Cleveland, OH 44115, p.fodor@csuohio.edu

Abstract: In this work the COMSOL Fluid Dynamics and Chemical Engineering modules are used to model the fluid flow through a microchannel based fuel cell. The particular design employed exploits the laminar nature of the fluid flow at small Reynolds numbers to keep the fuel and oxidizer confined in the vicinity of the corresponding electrodes, without the need for a proton exchange membrane (PEM). The performance of these cells is evaluated as a function of the aspect ratio of the channel used and the flow rates through it. Based on the reactants' consumption rates, the best performing cells are the ones with high aspect ratio operated at high Péclet numbers. The formation of a depletion boundary layer close to the electrodes of the cell is found to be the main factor limiting the efficiency of this type of cells.

Keywords: Microfluidics, membrane-less fuel cells, laminar flow, fluid dynamics.

1. Introduction

In the last decades, portable electronic devices such as cell phones, laptops, PDAs and electronic book readers have become prevalent in our society. Besides fueling a revolution in social media and in how information is distributed and gathered, these devices have also become an increasingly popular platform for applications in medical diagnosis, environmental monitoring, and military technology. As the performance of portable electronics devices, in terms of speed, memory and supported sensor platforms, continues to increase, so do their power requirements. Combined with the continuous trend towards miniaturization, this requires new energy storage technologies capable of providing the required energy densities. One such technology relies on developing miniaturized fuel cells. Besides a better energy density compared with current rechargeable battery technologies, the advantages of this approach include broader operating temperature ranges and the ability of

storing the chemical energy outside the cell and thus eliminating the recharge time.^{1,2}

Efforts in developing prototypes of small footprint fuel cells have already been undertaken.³⁻⁷ The primary component of a typical design is a rectangular microchannel with catalytic electrodes patterned on the sides or the top of the channel. The fuel (for example formic acid solutions or methanol) and oxidizer (oxygen saturated solution) streams are fed through T or V shaped connectors close to the corresponding electrode (Figure 1). While geometrically simple, the microchannel based design takes advantage of the laminar flow characteristics in the low Reynolds number regime. The lack of mixing between the fuel and oxidant streams, except for a diffusive region at the liquid – liquid interface, confines the oxidation of the fuel and the reduction of the oxygen reactions to the appropriate electrodes. In a regular fuel cell this is achieved by using a proton exchange membrane (PEM) which is permeable only to protons. The working life of PEM based designs is limited by functional issues, such as membrane fouling and drying out due to osmotic drag. Thus the design investigated provides not only a path for miniaturizing the fuel cell, but also a more robust approach by exploiting the lack of turbulent mixing to eliminate the need for a proton exchange membrane separating the liquid streams.

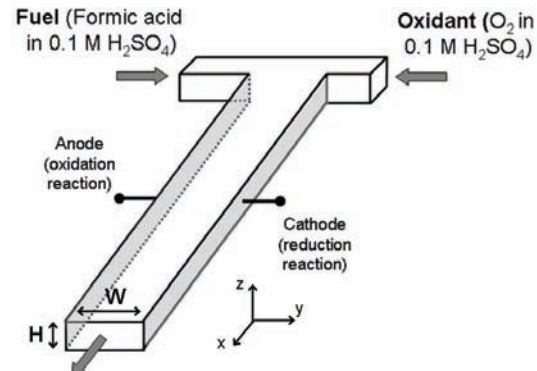


Figure 1. Typical design for a membraneless fuel cell based on laminar flow.

However, it has to be mentioned that the efficiency of these cells in terms of the reactant consumption rates can be quite low, i.e. a few percent.³ As discussed below, this is due to the formation of a boundary layer close to the electrodes, in particular the cathode, because of the limited mass transport that fails to replenish the reactants close to the catalytic electrodes.^{7,8} Making longer channels to allow the diffusion to replenish this depletion layer is not a solution since the diffusion also broadens the interface layer between the fuel and oxidizer streams leading to undesired reactant crossover. Within these constraints this work and previous computational analyses^{7,9,10} have focused on optimizing the efficiency of these cells.

2. Modeling in COMSOL Multiphysics

In this study the dependence of the performance of microchannel fuel cells on the aspect ratio and flow rate is evaluated. The cells are modeled as rectangular channels which confine the fuel and oxidizer streams. The concentration profiles for the typical T or V shaped inlet configurations used in experimental work are mimicked using mirror step functions for the fuel and oxidant concentrations. Typical parameters for the constants used in the simulations are listed in Table 1. The height H and width W of the channels are varied between 75 and 150 μm to obtain different aspect ratio channels, while the Péclet number is changed between 500 and 5000. For each set of H and W, and each Péclet number, the length L of the channel is limited to values for which the interface diffusion layer between the fuel and oxidizer streams does not extend to the opposite electrode. This ensures that the best cell efficiency can be achieved, while confining the reduction and oxidation reactions at the correct electrodes. In these simulations the fuel is assumed to be 0.5 M formic acid in 0.1 M H_2SO_4 aqueous solution, and the oxidizer is oxygen saturated 0.1 M H_2SO_4 aqueous solution.

2.1 Fluid dynamics

In order to simulate the fuel and oxidizer transport and consumption through the cell, first the flow fields in each structure are simulated using the COMSOL Fluid Dynamics module. This is done by solving the Navier – Stokes

Table 1: Typical parameters used in the simulations.

Parameter	Symbol	Value
Fluid density	ρ	$1 \times 10^3 \text{ kg/m}^3$
Fluid viscosity	η	$1 \times 10^{-3} \text{ kg/m}\cdot\text{s}$
Oxygen diffusion coefficient	D_O	$2 \times 10^{-9} \text{ m}^2/\text{s}$
Formic acid diffusion coefficient	D_{FA}	$5 \times 10^{-10} \text{ m}^2/\text{s}$
Oxygen inlet concentration	$c_{o,O}$	$2.5 \times 10^{-3} \text{ M}$
Formic acid inlet concentration	$c_{o,FA}$	0.5 M
Exchange current density for the reduction reaction	i_o	57 A/m^2
Overpotential at cathode	η_c	0.6 V
Channel width	W	$75 - 150 \mu\text{m}$
Channel height	H	$75 - 150 \mu\text{m}$

equations of motion for an incompressible Newtonian fluid.

$$\rho \left[\frac{\partial \mathbf{u}}{\partial t} + (\mathbf{u} \cdot \nabla) \mathbf{u} \right] = -\nabla p + \eta \nabla^2 \mathbf{u} \quad [1]$$

$$\nabla \cdot \mathbf{u} = 0 \quad [2]$$

Where \mathbf{u} is the velocity vector, ρ is the fluid density, η is the fluid, t is the time, and p is the pressure. The equations are solved for a steady state flow with no slip boundary conditions at all surfaces and zero pressure at the outlet. We have used a parametric triangular mesh generated across the inlet surface and then swept through the entire geometry. The minimum and maximum element sizes for the triangular mesh are $0.08 \cdot L_h$ and $0.04 \cdot L_h$, respectively (L_h is the hydraulic diameter of the channel).

2.2 Species transport and chemical reactions

Subsequent to obtaining the solution for the velocity field, for each of the species involved, i.e. fuel and oxidizer, the convection – diffusion equation is solved:

$$\frac{\partial c_i}{\partial t} = D_i \nabla^2 c_i - \mathbf{u} \cdot \nabla c_i \quad [3]$$

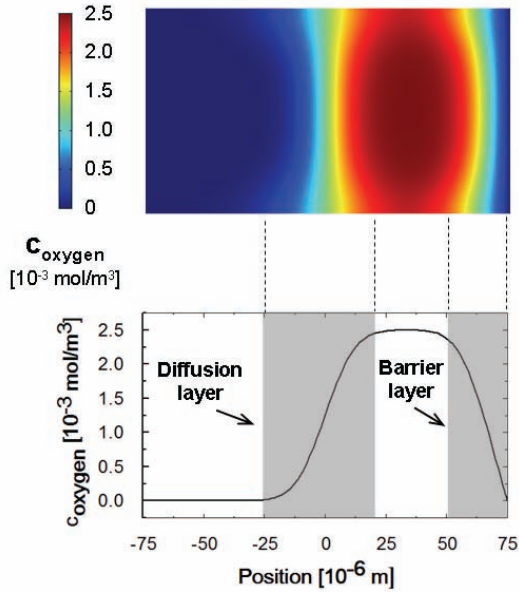


Figure 2. Concentration profile of the oxygen in a channel with $W = 150 \mu\text{m}$, $H = 100 \mu\text{m}$ and $\text{Pe} = 10^3$. The cut is taken at a distance $x = 0.25 \text{ L}$ from inlet.

In the above equation the index i indicates the fuel or oxidizer, and c_i and D_i are the corresponding concentration and diffusion constant. The concentrations of each species throughout the volume of the channel are obtained using the COMSOL Transport of Diluted Species module on a mapped mesh with minimum element size $1\text{-e-}6 \text{ m}$ and maximum element size $3.25\text{e-}6 \text{ m}$.

The chemical reactions at the catalytic surfaces and the consumption of the fuel and oxidizer are modelled using negative fluxes determined by the reaction rate k and concentration c . The rate of oxygen reduction at the cathode was calculated using the Butler – Volmer equation:⁷

$$k_O = \frac{i_0}{z \cdot F} \left(e^{-\frac{\alpha \cdot n \cdot F \cdot \eta_c}{R \cdot T}} - e^{-\frac{(1-\alpha) \cdot n \cdot F \cdot \eta_c}{R \cdot T}} \right) \quad [4]$$

where k_O - surface reaction rate for oxygen reduction, i_0 - exchange current density, z - valence, F - Faraday constant, T – temperature, $\alpha = 0.5$ - transfer coefficient rate, $n = 1$ – electron transfer number, $\eta_c = 0.6 \text{ V}$ – overpotential at cathode, and R – universal gas constant.

Given that the oxygen reduction rate is the

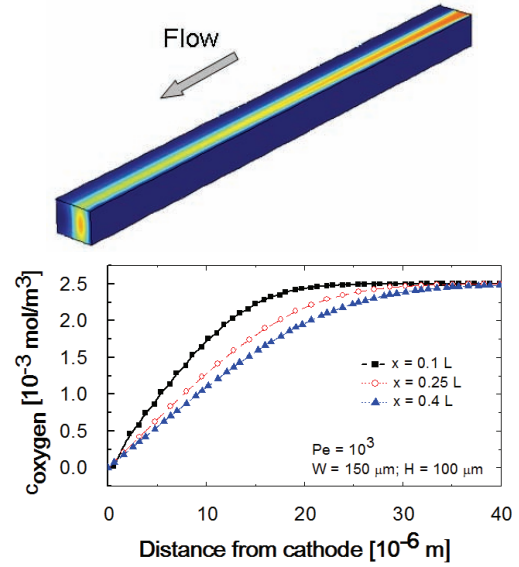


Figure 3. (Top) Surface plot of the oxygen concentration in the microchannel; (Bottom) Concentration line cuts close to the cathode at different positions along the channel.

limiting step,^{7,8} the reaction rate for the fuel is adjusted to maintain global charge neutrality, and the discussion below focuses on analyzing the performance of the fuel cells in terms of oxygen utilization.

3. Discussion

A typical oxygen concentration profile slice across the channel is shown in Figure 2. A few characteristics are immediately apparent. Firstly, at the interface between the oxygen saturated solution and the fuel stream, there is a diffusion layer that assumes the hour-glass shape characteristic to multi-stream laminar flow through rectangular channels. Close to the bottom and top walls, the rate at which the width of the diffusion region increases agrees well with the experimentally determined power law¹¹, $\Delta y \sim (D \cdot x)^{1/3}$, where D is the diffusion constant and x is the position along the channel. The broadening of the interface region as the streams move closer to the outlet is undesirable, due to the reactant crossover and the adverse effect on the performance of the cell associated with the fuel or oxidizer reacting at the incorrect electrode. Secondly, close to the cathode a depletion barrier layer is formed due to the consumption of

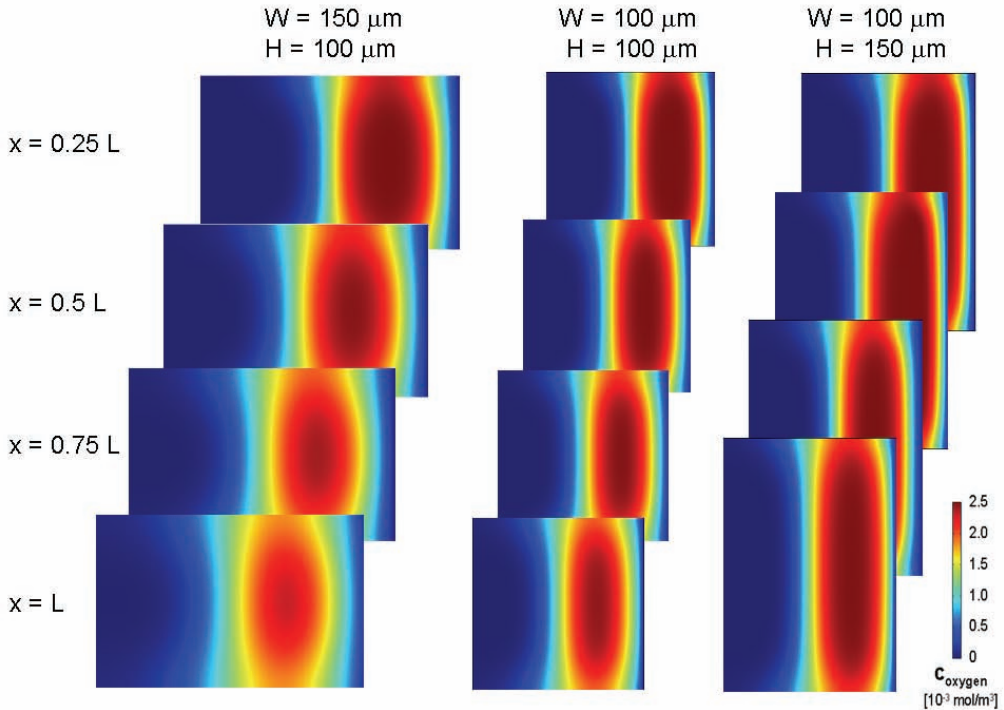


Figure 4. Oxygen concentration profiles at different positions along channels with aspect ratio 1.50, 1.00, and 0.66 respectively. For all the cases $\text{Pe} = 10^3$.

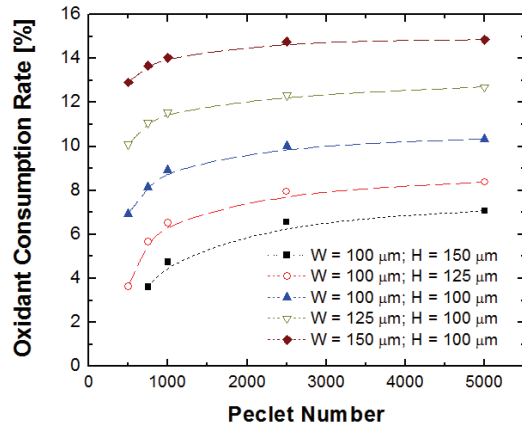


Figure 5. Oxidant consumption rate vs. Péclet number for different (W, H) pairs.

the oxygen. The width of the depletion layer (Figure 3 and 4) increases as the fluid moves along the channel, which is expected as more oxygen is removed from the stream by the reduction reaction occurring at the cathode. However, while the increase is steep at the beginning of the channel, it becomes less pronounced as the streams move along the channel, and thus a relatively large portion of the

oxidizer stream exits the channel without being used. This indicates that the main limiting factor in the performance of these cells is the mass transport close to the cathode, which in the absence of turbulent mixing relies only on diffusion to bring oxygen through the barrier layer close to the reacting surface. Additionally, the mass transport is also limited by the low oxygen concentration achievable, even in saturated solutions.

The amount of oxidant/fuel utilized is calculated by integrating across the inlet and outlet the fluxes of corresponding species. An analysis of the oxidant consumption rate when changing the width of the channel W while keeping the height H constant indicates that the efficiency of the cell increases monotonically as W becomes larger (Figure 5). Actually, within the sets of (W, H) used the most relevant geometrical parameter determining the performance of the fuel cells is the aspect ratio, with fuel cells with high aspect ratio consistently performing better. Also, designs with different widths and heights, but identical aspect ratios (Figure 6) behave identically in terms of reactant

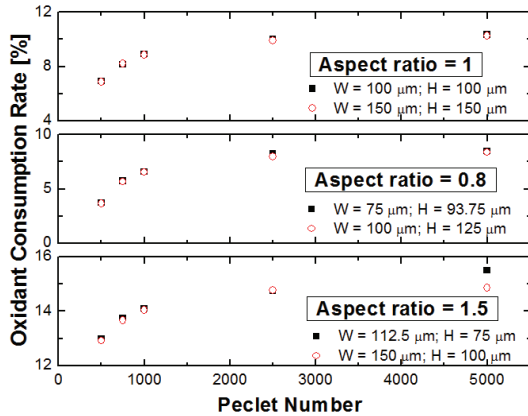


Figure 6. Oxidant consumption rate dependence on the aspect ratio.

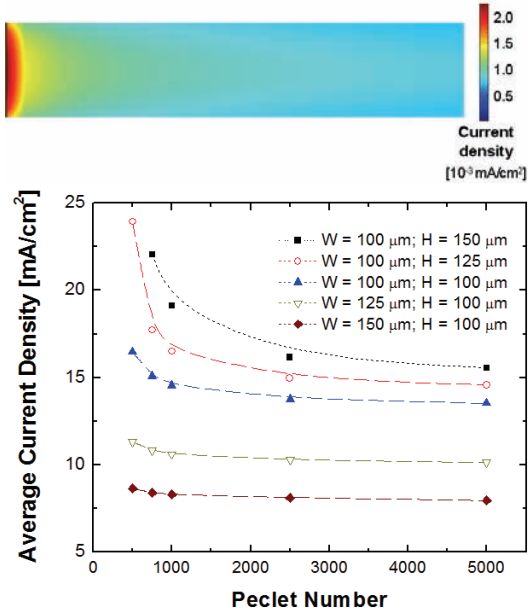


Figure 7. (Top) Simulated current density through the cathode; (Bottom) Aspect ratio dependence of the current density through the cell.

consumption. For high aspect ratio microchannels, the diffusive mixing region at the interface between the two liquid streams is narrower. This allows for the length of the microreactors to be increased without the adverse effect on performance associated with the reactants diffusing towards the opposite electrode. Operation of the fuel cells at high flow rates also contributes to better efficiencies as the oxidizer and fuel streams are pressed closer to the cathode and anode, respectively.

While using channels with higher aspect ratio is a strategy that addresses the reactants' crossover problem, and allows for an improved

performance, the efficiency of these cells is still relatively limited. Mapping the current density through the cathode (Figure 7) based on the amount of oxygen reacted at different points along it, indicates that a sizable part of the oxygen consumed is associated with reactions at the beginning of the microreactor. This supports the conclusion^{7,8} that ultimately the performance of this type of cells is limited by mass transport in the cathodic region. Increasing the flow rate (Péclet number) expands the region on the cathode across which the reduction reaction occurs as indicated by the drop in the average current density. While this is a viable strategy to increase performance, its use is limited by the realistic flow rates that can be used.

4. Conclusions

Simulations of fluid flow, species transport and surface reactions in microchannel fuel cells have been used to identify the geometrical and flow characteristics associated with efficient reactant consumption. High aspect ratio cells operated at high flow rates show the highest efficiency. In all the cases investigated the efficiency is limited by the formation of a reactant depleted region close to the catalytic electrodes. Thus future works in the development of more efficient cells exploiting this design will have to address the limited diffusion driven mass transport close to the reactive surfaces.

5. References

- Y. Vilenchik, E. Peled, and D. Andelman, “Kicking the oil addiction”, *Physics World*, January, 2 (2010).
- A. Kundu, J.H. Jang, J.H. Gil, C.R. Jung, H.R. Lee, S.-H Kim, B. Ku, and Y.S. Oh, “Micro-fuel cells – Current development and applications”, *J. Power Sources*, **170**, 67 (2007).
- E. Kjeang, N. Djilali, and D. Sinton, “Microfluidic fuel cells: A review”, *J. Power Sources*, **186**, 353 (2009).
- E. Choban, J.S. Spendelow, L. Gancs, A. Wieckowski, and P.J.A. Kenis, “Membraneless laminar flow-based micro fuel cells operating in alkaline, acidic, and acidic/alkaline media”, *Electroch. Acta*, **50**, 5390 (2005).

5. R. Ferrigno, A. D. Stroock, T.D. Clark, M. Mayer, and G. M. Whitesides, “Membraneless vanadium redox fuel cell using laminar flow“, *J. Am. Chem. Soc.*, **124**, 12930 (2002).
6. J.L. Cohen, D.A. Westly, A. Pechenik, and H.D. Abruña, “Fabrication and preliminary testing of a planar membraneless microchannel fuel cell“, *J. Power Sources*, **139**, 96 (2005).
7. R.S. Jayashree, S. K. Yoon, F.R. Brushett, P.O. Lopez-Montesinos, D. Natarajan, L.J. Markoski, and P.J.A. Kenis, “On the performance of membraneless laminar flow-based fuel cells“, *J. Power Sources*, **195**, 3569 (2010).
8. E.R. Choban, P. Waszczuk, and P.J.A. Kenis, “Characterization of limiting factors in laminar flow-based membraneless microfuel cells“, *Electrochim. Solid State Lett.*, **8**, A348 (2005).
9. A. Bazylak, D. Sinton, and N. Djilali, “Improved fuel utilization in microfluidic fuel cells: A computational study“, *J. Power Sources*, **143**, 57 (2005).
10. M. H. Chang, F. Chen, and N. S. Fang, “Analysis of membraneless fuel cell using laminar flow in a Y-shaped microchannel“, *J. Power Sources*, **159**, 810 (2006).
11. R. F. Ismagilov, A.D. Stroock, P.J.A. Kenis, and G. Whitesides, “Experimental and theoretical scaling laws for transverse diffusive broadening in two – phase laminar flows in microchannels“, *Appl. Phys. Lett.*, **76**, 2376 (2000).

6. Acknowledgements

One of the authors (i.e. J. D'Alessandro) was supported through a grant from the Cleveland State University Provost office.